Friction **12**(6): 1235–1249 (2024)
https://doi.org/10.1007/s40544-023-0803-1
ISSN 2223-7690
CN 10-1237/TH

RESEARCH ARTICLE

Prediction of ball-on-plate friction and wear by ANN with data-driven optimization

Alexander KOVALEV, Yu TIAN, Yonggang MENG*

State Key Laboratory of Tribology in Advanced Equipment, Tsinghua University, Beijing 100084, China

Received: 05 April 2023 / Revised: 15 May 2023 / Accepted: 07 July 2023

Abstract: For training artificial neural network (ANN), big data either generated by machine or measured from experiments are used as input to "learn" the unspecified functions defining the ANN. The experimental data are fed directly into the optimizer allowing training to be performed according to a predefined loss function. To predict sliding friction and wear at mixed lubrication conditions, in this study a specific ANN structure was so designed that deep learning algorithms and data-driven optimization models can be used. Experimental ball-on-plate friction and wear data were analyzed using the specific training procedure to optimize the weights and biases incorporated into the neural layers of the ANN, and only two independent experimental data sets were used during the ANN optimization procedure. After the training procedure, the ANN is capable to predict the contact and hydrodynamic pressure by adapting the output data according to the tribological condition implemented in the optimization algorithm.

Keywords: machine learning; deep learning; artificial neural network; mixed lubrication

1 Introduction

During the last decade, artificial intelligence (AI) has steadily progressed, starting from the computational statistical paradigms, to today's successful intelligent machines involving technologies such as object and sound recognitions, language translation, reliable image and sound generations, car and robot control, prediction and decision making [1]. Basically, machine learning (ML), as an important portion of artificial neural network (ANN), is a set of techniques, methods and algorithms aimed at providing and achieving an "intelligent final result" based on the analysis of the data used. Applications of novel ANN technologies in tribology can open new ways to solving difficult engineering problems effectively and providing new opportunities for future challenges (for a review see, e.g. Ref. [2]). Recent reviews on the application of ANN techniques in tribology [3–6] have prospected wide areas to which deep learning (DL) techniques can be efficiently applied. Also, an interesting idea proposed by Zhang et al. [7] is to establish a tribology database which would be useful for the preservation and dissemination of tribological research information within areas where ML and DL techniques are practised.

Mixed lubrication is a regime across the full fluid film lubrication and boundary film lubrication, and widely exists in most engineering tribosystems. Due to the complex mechanisms of interactions and mutual influence of physical phenomena existing in a mixed lubrication regime, there are no simple and unified general physical laws for prediction of friction and wear at mixed lubricated contacts. In general, the complex interactions in mixed lubrication are studied by either a numerical approach or a phenomenological one. A typical numerical approach is based on setting up a system of partial differential equations to define the state of the friction process with fluid lubrication of rough solid surfaces and elastic or elastoplastic

* Corresponding author: Yonggang MENG, E-mail: mengyg@tsinghua.edu.cn

contact mechanics of the rough surfaces. It allows to provide numerical solutions for wear [8–10] based on the idea of Patir and Cheng's average flow model [11], or by using the idea of wear dependent asperity contact pressure [10]. Many other implementations [12, 13], including the finite element method (FEM) and boundary element method (BEM) have also been proposed in recent years. Many tribological problem have been successfully modelled by means of FEM, such as contribution of elastohydrodynamics effect on friction [14], the influence of deformation model on the elasto-hydrodynamic lubrication modeling [15], application of FEM friction model for a problem of metal forming [16]. However, numerical modelling is not only computationally expensive due to its iterative nature, but also less reliable and correct than expectations because constants and parameters associated with the complicated mathematical equations as well as the boundary conditions are often poorly specified a priori. The phenomenological or analytical approach presumes the hypothesis of the physical laws describing the film thickness of lubricant [17], the rheological properties of lubricants [18], the stochastic approach to determine the contact deformation of asperities [19, 20], etc. The disadvantage of phenomenological or analytical approach is that the accuracy of any analytical equation involved in mixed lubrication, due to its simplified nature, is inadequate comparing with the real situations.

An aptitude of a neural network system can provide a non-linear relationship between input parameters and output data, which is able to model the operation of mechanical systems. Recently, the ANN technique has very often been used as a tool for the analysis of wear test data [21–26]. Many dependencies have been established in the form of ANNs, where the material or mechanical properties [25–27], structural or surface parameters [28, 29] are used as input data for ANN [6, 30]. However, in most cases only one functional property of ANNs is realized, which is to produce an approximation fit between input and output data. ANN has therefore been used as a universal function approximator. A non-linear functional regression fit can be easily implemented in terms of ANN modelling and applied to tribology tasks, and this approach has been extensively studied by Argatov [6]. The comparison investigation between physical and machine learning modeling to predict fretting wear volume was done by Baydoun et al. [31].

In contrast to the application of conventional simple ANN, the advanced type of ANN is now being developed. The aim is to move away from direct approximation, to identify the features of the physical phenomena under consideration and to design the ANN structure to evolve the features related to the problem under investigation. One of the interesting and promising type of ANN is physical-informed neural network (so called a PINN). Perhaps, the first introduction of PINN was done by Raissi et. al. as an ANN modelling to solve non-linear partial differential equations [32]. Using this type of ANN investigation many physical problems were "solved" by the proposed PINN. There are many classical physics laws were incorporated and appropriate solutions were found for the problems as the velocity and pressure fields for the fluid mechanics [33], discovery of non-linear elastoplastic behavior of solids [34] and data-driven parametric partial differential equations [35, 36]. The SciANN wrapper [37] (written in Python language and includes all the necessary functions of Tensorflow/Keras packages related to PINN design) can be used to focus the ANN construction on finding an approximation for a differential or partial differential equation. The role of an error approximation techniques that realized in PINN architecture has been well studied by Zubov et al. [38]. The ability to apply the PINN techniques to lubricated contact has been investigated by Almqvist [39] to solve the Reynolds boundary problem, by Wang and Tsai [40] to predict the maximum pressure in thermos-hydrodynamic contacts, by Marian [41] to predict the film thickness in EHL contact. In most cases, the numerical data from FEM modelling was used to train the ANN, in such a case, the ANN will only be a replica of the FEM proposed solution.

It should be noted that there exists another physical-informed neural network (also called PINN), introduced by Nascimento and Viana [42, 43] and Dourado and Viana [44]. Despite the same sounding title, the idea used is quite different. These authors have used the specially modified recurrent neural cell to construct the recurrent neural network (RNN) with embedded specific physical law to estimate the time-dependent physical process, such as a cumulative

damage process in a mechanical system. This approach will lead the researchers to develop the digital twin based on the ANN principles.

In fact, the PINN method inherits an idea of an adaptive learning method for NN that was proposed about 10 years ago [45], where one of the ideas is to replace the traditional method of minimizing the error by the specific equation that provides the connection to the studied process. In other words, to implement the physical law in the adaptation algorithm. Moreover, the idea of implementing the physical laws or equations was introduced more than 20 years ago, see for example Oussar and Dreyfus [46] or Forsell and Lindskog [47], which described a general methodology for a "gray-box" or semi-physical modelling implemented in neural networks. The semi-physical NN modelling for one of the interesting tribological problems has been presented by Haviez et al. [48] in 2015. The authors have shown that the fretting wear evolution can be estimated by ANN without using of the back-propagation learning algorithm and without any regularization method.

The aim of this paper is to show that instead of the "black box mystery", ANN modelling in a tribological task could be more fruitful if the ANN model is designed according to the real physical phenomena governing the friction process under consideration. Here we show how the modified optimization algorithm embedded in the ANN training process allows us to evaluate the "hidden" or unknown tribological functionalities, especially for the ball-on-plate friction scheme, but the considered ANN method is not limited by the chosen tribological test scheme and can be applied to analyze any other friction and wear data. The novelty of the proposed research is that we have constructed the ANN as a set of parallel multylayer perceptrons (MLPs), each corresponding to the specific function to be studied, and the training procedure is enforced by a modified loss function consisting of physical constraints and simulated constitutive laws.

2 Brief descriptions of ANN architecture and optimization procedure

A brief overview of the basic concepts of the structure and competence of neural networks [49] is presented in this section, with particular emphasis on the features of the training procedure that can be useful in modelling (or learning) tribological phenomena.

2.1 Feedforward neural network structure

In context of computing system ANN consists of interconnected units (neurons) that processes information by responding to external inputs, relaying information between each connected unit. The process requires multiple passes at the input data to find connections and derive meaning from undefined data to deliver a data signal to the output data. For a single layer with inputs $\boldsymbol{x} \in \mathbb{R}^m$ and outputs $\boldsymbol{y} \in \mathbb{R}^n$ we can write the approximation equation as

$$\boldsymbol{y} = \sigma\left(\boldsymbol{W}_i \boldsymbol{x} + \boldsymbol{b}_{i-1}\right) + \boldsymbol{b}_i \tag{1}$$

where $\boldsymbol{W}$ is the matrix of weights at i level of ANN, $\boldsymbol{b}$ is the bias matrix and, σ is the activation function.

Each input node in ANN has an associated weight $\boldsymbol{W}$ that represents the relative strength or the importance of the input. An initial value is assigned to each weight, but these values are not static. As the neuron is trained, as will be explained below, the weights are continuously adjusted to obtain a more accurate result and it is through these continuous adjustments that the neuron learns. A bias $\boldsymbol{b}$, which has a constant initial input and is updated during training like weights, is simply added to the weighted sum of each node.

The transfer or activation function σ of each processing neuron is a mathematical formula that determines the output y of the neuron. Its purpose is to prevent outputs from reaching very large values which can inhibit training. A number of transfer functions are used in practice, i.e. the linear, non-linear (sigmoid) and binary threshold functions. Lastly, the output y corresponds to the solution of a problem, and usually needs to be transformed into a format suitable as input to another neuron or as a piece of information that is understandable to the user.

2.2 Training (or learning) loop of ANN

Training the ANN is the most important part of the "learning" process. Actually, the training procedure is an application of specific algorithms that have been

developed for ML. Indeed, the training of ANNs looks like a "miracle" at first sight, but this process is based on real human learning when the desired goal has to be achieved in common live cases. Each time we make a mistake, we train to correct the activity, which minimizes the gap to the desired outcome. We do it again, perhaps many times, until our action completes our goal. In a case of ANN, this repeat loop is called an Epoch, the correction of weights in backward way is called a backward propagation process. The general scheme of ANN training is showed in Fig. 1.

A popular method of training an artificial neuron is by error correction: the difference between the neuron's actual output y and the correct output t, defined to be the desired output, is calculated. This difference is also known as a learning error. If the response at the output is incorrect then the neuron weights should be changed so that it is more likely to produce the correct response the next time that the input stimulus is presented. Neural network training essentially involves a loss function. The value of the loss function gives a measure of how far from the perfect performance of the NN is on a given dataset.

At present, a variety of loss (or cost) functions have been proposed and used for classifying and regressing data by means of ANN. In our research, we used the following two commonly used loss functions as mean square error (MSE) and mean absolute error (MAE):

$$\mathcal{L}(\mathrm{MAE}) = \frac{1}{N}\sum|u-\hat{u}| \tag{2}$$

$$\mathcal{L}(\mathrm{MSE}) = \frac{1}{N}\sum(u-\hat{u})^2 \tag{3}$$

where $\hat{u}$ is a predicted value and u is the real value of the function. MSE is a differentiable function that makes it easy to perform mathematical operations in comparison to a non-differentiable function like MAE.

Once the loss function is selected, the weight set have to be recalculated based on the appropriated error set. This is implemented in the training loop of the ANN by the use of specific algorithms that allow the input of the error data to the NN in a fast way. These set of algorithms are called as optimizers [50]. There have been controversial results in the literature about the characteristics of available optimization methods. Therefore, there is a need for exploring which optimization method should be chosen for a particular task. Commonly used optimizers for linear/non-linear regressions are gradient descent (GD), stochastic gradient descent (SGD), RMSProp, ADAM (adaptive moment estimation) and many others. The use of a specific optimizer depends on the architecture of the ANN and the purpose for which it is used. In our study, the ADAM algorithm [51] was used because it works quickly and perfectly to evaluate the non-linear regression for the function of interests.

The general form of optimization process is described by Eq. (4). In a case, trying to approximate the function $D(x)$ with respect to the network of neurons $\mathcal{N}(x,\boldsymbol{W},\boldsymbol{b})$, the optimization rule using the ADAM algorithm is as Eq. (4):

$$(\boldsymbol{W}^*,\boldsymbol{b}^*) = \mathrm{ADAMargmin}\mathcal{L}(\boldsymbol{W},\boldsymbol{b}) = D(\boldsymbol{x}) - \mathcal{N}(\boldsymbol{x},\boldsymbol{W},\boldsymbol{b}) \tag{4}$$

where x is a set of training points, $\boldsymbol{W}$ is a matrix of weights, and $\boldsymbol{b}$ is a matrix of biases.

A natural advantage of the optimization technique is that, since all loss functions (MSE or MAE) contain the form of error minimization computed as part of the ADAM adaptivity routine, they are not restricted to the general form of Eqs. (2) and (3) for a given values

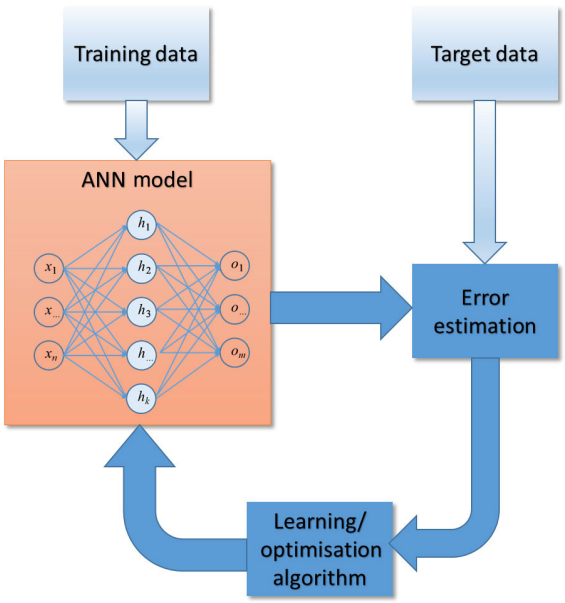

Fig. 1 Diagram of training/learning loop for a conventional ANN.

u and $\hat{u}$, it could be extended to use an analytical equation or function u with respect to the expected target function value $\hat{u}$. Exactly this feature for modifying the loss function $\mathcal{L}(\boldsymbol{W},\boldsymbol{b})$ has been realized in this study.

In the study, each function corresponding to the process under investigation was represented by its neural network. The experimental data set, if available, was fed into the loss function to evaluate the expected target value. Because the loss function may have multiple terms, each term must correspond to a particular neural network to determine the part of the loss that contributes to the total loss, we have examined the ability of the joint neural networks to be able to predict the output data when the error estimation is shared between the neural networks.

3 Modelling of mixed lubrication

In order to illustrate the potential of ANN with data-driven optimizer for predicting complex friction problems, in this section we have considered two cases where the ability and suitability of ANNs for estimating and predicting friction and wear under mixed lubrication is investigated.

3.1 Friction force under lubricated condition

Following the Bowden and Tabor [52], it is both reasonable and physically correct to consider the friction force between two solids as the product of the interfacial strength within the area of real contact.

As a general simplification, the friction force can be expressed as the sum of three components contributing to the total friction force.

$$F = F_{\mathrm{h}} + F_{\mathrm{b}} + F_{\mathrm{s}} \tag{5}$$

where F_{h} is a contribution of hydrodynamic shear force, F_{b} is the boundary friction and F_{s} is caused by the solid–solid contact.

In simple case for a Newtonian liquid, the shear force is the integration of the viscous shear stress t_{h} over the fluid area A_{h} that can be written as

$$F_{\mathrm{h}} = \int_0^{A_{\mathrm{h}}} \frac{\eta u}{h}\mathrm{d}A = \int_0^{A_{\mathrm{h}}} \mu_{\mathrm{h}} p_{\mathrm{h}}\mathrm{d}A \tag{6}$$

where η is the viscosity parameter, u is the velocity, μ_{h} is shear stress coefficient, and p_{h} is a hydrodynamic pressure. However, it is known that due to the rheological properties of the lubricant, the hydrodynamic pressure is not constant and can follow an exponential law [53].

Boundary friction F_{b} exists due to the presence of the boundary contact area A_{b}, which is chemically formed by the molecular layer of lubricant [54]. In the initial state of the lubricant contact, A_{b} is located around the real contact areas A_{r}, which are within the nominal contact area A_{n}. In the running process, the boundary friction surface is created by the formation of the boundary lubricant layer with the thickness of a single molecule. In general point of view, the boundary friction force can be expressed as Eq. (7):

$$F_{\mathrm{b}} = \int_0^{A_{\mathrm{b}}} \mu_{\mathrm{b}} p_{\mathrm{b}}\mathrm{d}A \tag{7}$$

where μ_{b} is boundary shear coefficient, and p_{b} is an external pressure applied on the boundary area A_{b}.

The main contribution to volumetric wear is due to the direct contact of surface irregularities, which are also present in lubricated contact. The set of direct solid–solid contacts forms a real contact area A_{r} within which the removal process contributes to the friction force F_{s}.

Using the above representation of the forces acting, the friction force F_{s} due to solid–solid interaction can be written analytically as the integration of pressure over the corresponding area domain multiplied by the shear stress within

$$F_{\mathrm{s}} = \int_0^{A_{\mathrm{s}}} \mu_{\mathrm{s}} p_{\mathrm{s}}\mathrm{d}A \tag{8}$$

where μ_{s} is the solid–solid shear strength coefficient, and p_{s} is the external pressure applied to the real contact area (or solid–solid contact A_{s}).

As noted in Ref. [55], finding a solution using numerical approximation methods requires large amount of computational time that are largely dependent on solving the elasto-hydrodynamic (EHD) equations in the usual iterative manner. The use of an ANN methodology negates the excessive computational time of the numerical solution while maintaining accuracy. In our research we will illustrate that the general

relationships as Eqs. (5)–(8) are enough to make the ANN modelling to get the reasonable result that can be used for deep understanding of the relationships and interrelationship between friction properties.

3.2 Wear rate and contact pressure

In this investigation of friction of lubricated contact, the wear is considered as the change of surface geometry during the friction. The simplest and widely used law of wear process is the Archard wear law [56] that was used in ANN modelling to estimate the contact pressure. The Archard wear law presumes that between wear volume V and normal load L exists a linear dependence in a form

$$V = k\frac{L}{H}s \tag{9}$$

where s is the sliding distance, H is the hardness of the material, and k is the wear coefficient. One of the most commonly used parameters of wear is a wear rate, expressed in relation to time t as

$$\dot{w} = \frac{\mathrm{d}V}{\mathrm{d}t} = k\frac{L}{H}\frac{\mathrm{d}s}{\mathrm{d}t} = k\frac{L}{H}\frac{\mathrm{d}s}{\mathrm{d}t} \tag{10}$$

Equation (10) presumes the linear dependence between wear and sliding distance. However, in most of cases, this dependence is not linear as for lubricated contact of metals [57, 58], and for polymer materials [59] as well. The relation between wear rate and contact pressure is used in our research because the friction force is roughly proportional to the normal stress within the contact area caused by normal force applied [60, 61].

The application of ANN techniques for evaluation of non-linear mechanisms of wear, prediction of volumetric wear [62] and wear coefficients [63] was already published. The main assumption of the proposed applications of ANN is that the operating friction parameters, such as pressure, velocity and others, have been used as an input data for a simple straightforward architecture of ANN. This type of ANN allows the establishment of non-linear dependencies between input and output data as volumetric wear or wear coefficient. Unfortunately, the non-linear dependency discovered by conventional ANN architecture is valid for a given friction parameters and cannot be extended to other experimental conditions. This is because the training of ANN does not take into account the characteristics of the friction/wear properties as specific features of the friction and wear process. The features have to be extracted from experimental data by the "learning" process and the final prediction has to be made based on the feature properties but not on the raw experimental data. It can be realized in our ANN with complex architecture that can do this, as that it illustrated in Section 4.2.

4 Results and discussion

A simulation model of ANN is programmed in Python to describe the wear and friction evolution. The specific framework as Tensorflow and Keras have been used to develop ANNs according to the architecture evaluating the mechanism of friction and wear considered.

4.1 An experimental data set of friction and wear

In this paper we used experimental data of lubricated point contact during normal running-in process performed by Zhang et al. [64]. The tribology experiments were carried out on a universal tribometer manufactured by Rtec Instruments (USA). The triboscheme as a sliding friction with lubricant for a steel ball against a steel plate, both are GCr15 bearing steel, has been used in experiments. The wear coefficient GCr15 steel is accepted as 2.0×10^{-5} mm^3/(N·m) [65] with hardness of 60 HRC.

The experiments were carried out with an external load of 20 N, corresponding to a Hertz pressure of about 1 GPa and a contact radius of 94 mm. The slip distance was set to 5 mm at a constant speed of 20 mm/s.

The base oil polyol ester (POE) with dynamic viscosity of 0.031 Pa·s was used as the lubricant.

The White Lite interferometer built into the tribometer was used to measure the surface change of a tested samples. The 3D image of the surface can be created with nanometer resolution using this optical method, which was independent on the friction tests. The estimation of the volume of wear and the rate of wear was carried out by comparing the bearing areas

curves of the worn surfaces, and this approach is also described in Ref. [64].

4.2 ANN set up for wear rate prediction

In this section we illustrate the ANN with the capability of evaluation of "unknown" dependency between wear rate, time, and contact pressure. We have proposed to use a multi-layer perceptron for each function that acts in a parallel way in the friction process under consideration. In this case, the ANN architecture can be constructed as a set of parallel "strings" (MPLs) bounded by the same input data and physical constraints.

To evaluate the contact pressure in terms of complex ANN with "a string structure", the wear rate ($\dot{w}$) and pressure (p) can be represented as two independent MLPs. Each of MLP consists of several densely connected layers. The loss function implemented into optimization algorithms is the same for both MLPs. This ANN structure provides the link between the MLPs by means of collocation points (input data, first layer) and by the "shared" error data, resulting in the correlation of different quantities of interest (output layers for wear rate and contact pressure). The schematic representation of the ANN structure in Fig. 2 is shown.

Since friction is a time-dependent process, time (t) has been chosen as an input variable for both MLPs. The set on neurons in the input layer is equal to the time series points, and this set of points are collocation points for the output layers for both MLPs. The functions of wear rate and contact pressure should be represented in terms of NN as

$$\hat{\dot{w}}(t) \mapsto \mathcal{N}_{\mathrm{w}}(t, \boldsymbol{W}, \boldsymbol{b}) \tag{11}$$

$$\hat{p}(t) \mapsto \mathcal{N}_{\mathrm{p}}(t, \boldsymbol{W}, \boldsymbol{b}) \tag{12}$$

The loss function to evaluate the error during the training algorithm is

$$\mathcal{L} = \left|\dot{w} - \hat{\dot{w}}\right| + \left|p - \hat{p}\right| \tag{13}$$

The loss function consists of two terms. The first one denotes the difference between experimental wear rate data $\dot{w}$ and the data proposed by $\hat{\dot{w}} = \mathcal{N}_{\mathrm{w}}(t, \boldsymbol{W}, \boldsymbol{b})$, the second one is the condition to estimate the difference between NN for a pressure $\hat{p} = \mathcal{N}_{\mathrm{p}}(t, \boldsymbol{W}, \boldsymbol{b})$ and nominal error condition in the form

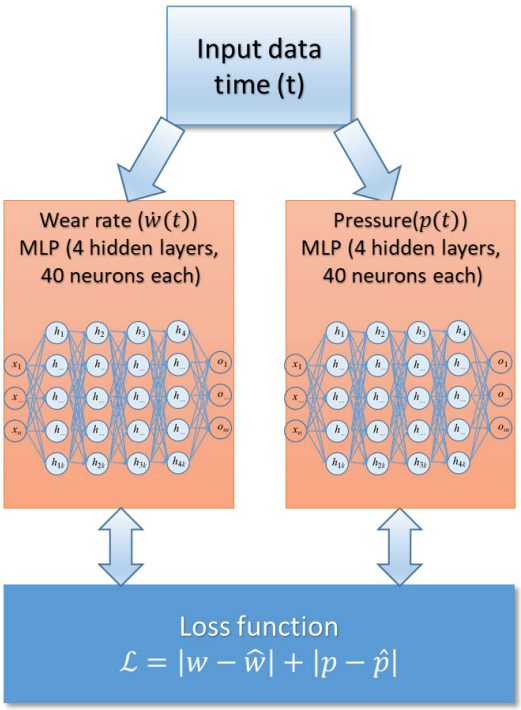

Fig. 2 ANN network structure for evaluation of wear rate and shear pressure. A 4-layer neural network with 40 neural units and hyperbolic tangent activation function was chosen for both MLP. The same loss function was used for updating the weights and biases for both MLP.

$$\| \circ \| = \begin{cases} \dot{w} - \hat{\dot{w}} \\ k\dot{w} \cdot \mathcal{N}_{\mathrm{p}}(t, \boldsymbol{W}, \boldsymbol{b}) - \hat{\dot{w}} \end{cases} \tag{14}$$

Note that while the input data (a time series) are the same, the optimization model is defined with two targets, one of which is driven by the set of experimental data $\dot{w}$, and the second one is adopted by the intermediate data of $\hat{\dot{w}}$ and the predicted data of $\hat{p}$ during the training (learning) procedure. Exactly this feature provides the ANN to evaluate the "unknown" functionality as a contact pressure.

The second formula in Eq. (14) represents the error calculation between the wear rate predicted by the MLP for the contact pressure $\hat{p} = \mathcal{N}_{\mathrm{p}}(t, \boldsymbol{W}, \boldsymbol{b})$. The point is that $\hat{p}$ is initially unknown and the output data is initialized as a set of random values. However, during the training process (also called the learning process), the ANN tries to revise the randomly initialized data according to an analytical way proposed

by error functions (Eq. (14)). These functions have the same experimental data set as the wear rate data ($\dot{w}$). This means that the calculated error is the same for two independent MLPs. The adaptation of ($\boldsymbol{W}$, $\boldsymbol{b}$) to the new set of output data takes place in an identical way. At the end of the ANN training process, the two output datasets (wear rate and contact pressure) are generated, each corresponding to the owner of its MLP ($\hat{w} = \mathcal{N}_w(t, \boldsymbol{W}, \boldsymbol{b})$ and $\hat{p} = \mathcal{N}_p(t, \boldsymbol{W}, \boldsymbol{b})$). The result of training ANN (for structure presented in Fig. 2) for evaluating the wear rate and the contact pressure is shown in Fig. 3.

The effect of the number of layers and the number of neurons was empirically investigated. We have tested three types of MLP structures with 2, 4, and 6 dense layers. All of them have shown the similar pattern of output wear rate and pressure data. The 4-layer structure is the best choice because the loss function has a smooth curve with no oscillation or distortion. The influence of neurons per layer was also examined. We have tested structures with neurons ranging from 20 to 80 per layer. It has been observed that the growth of neurons leads to an increase in computing time without improving the accuracy. The 40 neurons were chosen because the loss error converges to zero around 100 epochs.

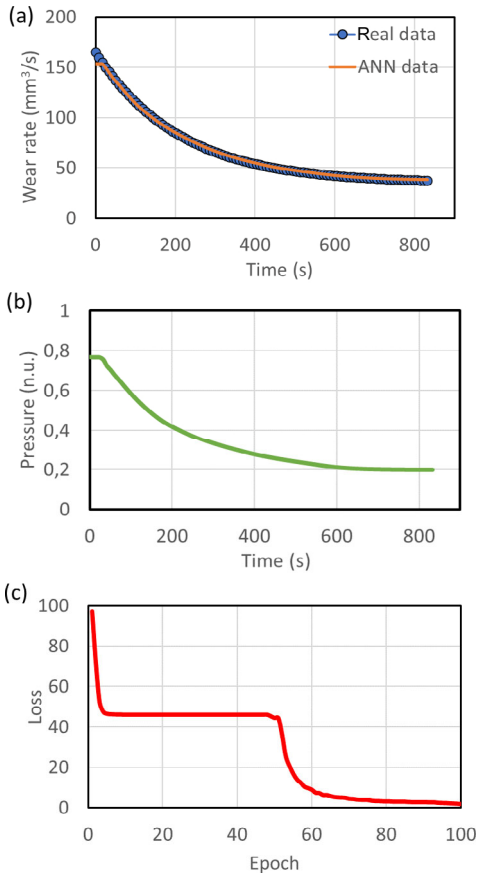

Fig. 3 Results of training ANN (for architecture in Fig. 2) for evaluation of wear rate and contact pressure. (a) Comparison of experimental data (blue line) and ANN prediction (orange line); (b) predicted shear pressure, "n.u." is a normalized unit; (c) the data of the loss function calculated at each epoch loop.

The special functions and parameters implemented in the Tensorflow/Keras framework were used to optimize the training procedure. There are "Batch size" set to 64 per gradient update for a batch optimization procedure, "Adaptive weights" set to 100 for a regularization procedure, and "Adaptive learning rate" initially set to 0.001. This set of optimization parameters allows us to perform fast and reasonable training of the ANN.

One immediate observation (see Fig. 3(a)) is that the curve of predicted wear rate completely fits the experimental data. It means that the constructed ANN is able to perform the prediction without overfitting or other factors affecting the distortion of output data. The contact pressure (see Fig 3(b).) was evaluated by ANN based on the error data involved in calculating the weight and biases for updating the state of MLPs. As it is seen, the general pattern of the $p_s(t)$ function is similar to the curve of $\dot{w}(t)$ that allow us to note that prediction of contact pressure is reasonable and corresponds to the analytical Eq. (10).

Figure 3(c) illustrates the loss function history of the ANN training. The first three epochs correspond to the identification of a stable initial error value, which is used as a reference point to minimize the difference between the expected value $\hat{w}$ and experimental $\dot{w}$ of the wear rate. The loss function history has a step wise pattern that can be attributed to the double MLP structure of the ANN. The smooth shape of the loss curve can be explained by the fact that we have found the correct number of layers and neurons within them, and have identified appropriate hyperparameters to perform accurate training. It was observed that 100 epochs of training were sufficient to bring the loss close to zero approximately.

4.3 ANN setup for prediction of friction data for lubrication contact

As a second example, we show here how the ANN

with data-driven optimization problem allows to evaluate two "hidden functionalities" in the same learning loop, using the two independent data sets on the same collocation points represented by a time sequence.

In the developed ANN model of friction under lubrication condition it is assumed that the external load L is transmitted by the bearing areas of hydrodynamic (A_h) and solid (A_s) contacts. Contacts with boundary friction F_b were assumed to be part of the solid contact, because although the frictional force is significantly reduced in these areas, the external pressure acting in the boundary area (p_b) is the same as that in the solid–solid contact. This approximation is realistic if the molecular boundary layer is assumed to be incompressible. The modelling of a mixed lubrication regime where the hydrodynamic pressure and the solid contact pressure allows to investigate the main characteristics of the lubricated contact have been investigated numerically for various cases [8, 9].

The proposed ANN structure with a set of MLPs for the evaluation of the hydrodynamic and solid contact pressure must have separated MLPs approximating the wear rate $\hat{w}$, contact pressure $\hat{p}_s$, hydrodynamic pressure $\hat{p}_s$ and friction coefficient $\hat{f}$ as the following:

$$\hat{w}(t) \mapsto \mathcal{N}_w(t, \boldsymbol{W}, \boldsymbol{b})$$

$$\hat{p}_h(t) \mapsto \mathcal{N}_h(t, \boldsymbol{W}, \boldsymbol{b})$$

$$\hat{p}_s(t) \mapsto \mathcal{N}_s(t, \boldsymbol{W}, \boldsymbol{b})$$

$$\hat{f}(t) \mapsto \mathcal{N}_f(t, \boldsymbol{W}, \boldsymbol{b})$$

Figure 4 shows the ANN consisting of four MLP for each evaluated function. In general, this multi-MLP feed-forward NN is capable of approximating unknown dependencies. However, when examining the proposed structure of ANN, the inaccuracy of approximation has been observed several times. Usually, it can be caused by lack of deterministic relationship between input and output data, insufficient number of layers and hidden units, insufficient training for a case of estimating two unknown functions. To overcome observed inaccuracy, the special Tensorflow/Keras functions have been used to improve the repeatability. The main ones were "batch optimization", which was implemented to specify the number of samples processed before updating the model, and "adaptive weights" to force the scale weights to fit the shape of the weight tensor. The number of epochs was doubled compared to the ANN described in Section 4.2, and the number of neurons was up to 80, the activation function has left a hyperbolic-tangent function as in the previous example.

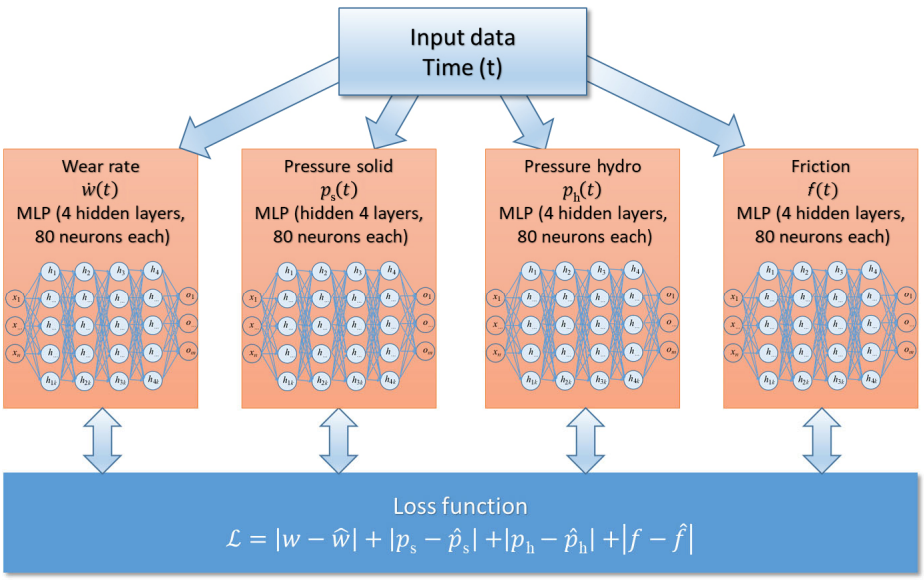

Fig. 4 ANN structure for evaluation unknown hydrodynamic pressure $p_h(t)$. A 4-layer neural network with 80 neural units and hyperbolic tangent activation function was chosen for MLPs representing the wear rate $\dot{w}$, contact pressure p_s, hydridynamic pressure p_h, and friction coefficient f. The time data are used for all MLPs as an input data.

It allows to reach a repeatability of about 70%. It is obvious that the ANN structure should be improved or modified in future implementations.

Following the procedure described in Section 4.2, the MLP for evaluating the wear rate $\hat{\dot{w}} = \mathcal{N}_{\mathrm{w}}(t, \boldsymbol{W}, \boldsymbol{b})$ is supported by the experimental data $\dot{w}$ by means of error calculation as $\mathcal{L}_{\mathrm{w}} = \left|\dot{w} - \hat{\dot{w}}\right|$. The contact pressure p_{s} is estimated by approximating $\hat{p}_{\mathrm{s}}(t) \mapsto \mathcal{N}_{\mathrm{s}}(t, \boldsymbol{W}, \boldsymbol{b})$ with the loss function $\mathcal{L}_{\mathrm{p}} = kv \cdot \mathcal{N}_{\mathrm{p}}(t, \boldsymbol{W}, \boldsymbol{b}) - \dot{w}$. The hydrostatic pressure p_{h} is also approximated by MLP $\hat{p}_{\mathrm{h}}(t) \mapsto \mathcal{N}_{\mathrm{h}}(t, \boldsymbol{W}, \boldsymbol{b})$ and uses the simplified relation for a friction coefficient, where boundary friction area is combined with solid contact

$$f = \frac{1}{L}\int_0^{A_{\mathrm{h}}} \mu_{\mathrm{h}} p_{\mathrm{h}} \mathrm{d}A + \frac{1}{L}\int_0^{A_{\mathrm{s}}} \mu_{\mathrm{s}} p_{\mathrm{s}} \mathrm{d}A \tag{15}$$

As it seen, there is no physical law on how the pressures change during the friction process in the governing Eq (15). For the prediction to be correct, it is necessary to provide the equation that links the hydrodynamic pressure and the contact pressure. The simple law for this is pressure equilibrium in the form $P_{\mathrm{H}} = p_{\mathrm{s}} + p_{\mathrm{h}}$, where P_{H} is the Hertz contact pressure applied to the entire nominal contact area that provided by the experimental conditions. The next point is that during the running-in process, the frictional force is affected by a series of relaxation phenomena occurring in the nominal contact area and caused by various factors. Bowden and Tabor [52] proposed to use the logarithmic relationship between contact area A_{r}, interfacial normal stress t_{n} and state variable f accounting such a transformation, Rice and Ruina [60, 66] considered the exponential laws between friction force F and state variable f, contact area A, contact stress s and velocity u. According to the above hypotheses, the behavior of the pressure distribution over time can be expressed in differential form as Eq. (16):

$$-\frac{\mathrm{d}p}{\mathrm{d}t} = k_{\mathrm{p}}(p - p_0) \tag{16}$$

where k_{p} is a rate constant related to the pressure distribution and p_0 is an initial value of pressure. The real experimental data of friction coefficient f [64] has been used in the data-driven optimization problem as a second data source. In our study for estimating the pressure distribution, we expected the ANN prediction to be in the form close to Eq. (16).

Considering that the objective is to determine the unknown solid contact pressure p_{s} and hydrodynamic pressure p_{h}, the set of loss functions has been set up as Eq. (17):

$$\|\circ\| = \begin{cases} \dot{w} - \hat{\dot{w}} \\ kv \cdot \hat{p}_{\mathrm{s}} - \dot{w} \\ \hat{p}_{\mathrm{s}} - \hat{p}_{\mathrm{h}} - P_{\mathrm{H}} \\ A_{\mathrm{s}}\hat{p}_{\mathrm{s}} + A_{\mathrm{h}}\hat{p}_{\mathrm{h}} - \hat{f} \\ f - \hat{f} \end{cases} \tag{17}$$

The ADAM optimizer has been used to perform the simulation with the constraints given in Eq. (17). This set of constraints, implemented in an optimization loop, allows the problem of neural surrogation to be solved, where in this form the error bounds for each function represented in terms of the MLP prediction, for used functions depending on the time $\dot{w}(t), p_{\mathrm{s}}(t)$, $p_{\mathrm{h}}(t), f(t)$ on unknown (or all) parameters can be computed by summing the error bounds from the individual function estimates. This gives an overall expected error in the mixed lubrication representation by the equations used, which can be shown to be proportional to the error in the dependent variables of the functions.

The results of the pressure evolution prediction are shown in Fig. 5, where 200 epochs were chosen to obtain the fastest and best performance.

The pressure prediction results are presented in a non-dimensional form. This makes it possible to analyse the friction behaviour in relation to the nominal contact pressure. Figure 5(a) shows that at the beginning of the friction test, the hydrodynamic pressure P_{H} contributes slightly to the frictional force. During the friction test, the effect of the hydrodynamic effect increases significantly and becomes dominant at approximately 600 s of duration. In contrast to p_{h}, contact pressure p_{s} is a major effect at the start of the test and decreases with time. In fact, such a predicted behaviour of a lubricated contact generally corresponds to the mixed lubrication regime.

The main feature revealed by ANN is that the contact pressure p_{s} and hydrodinamic pressure p_{h} are non-linear and evolve in apposite way due to the

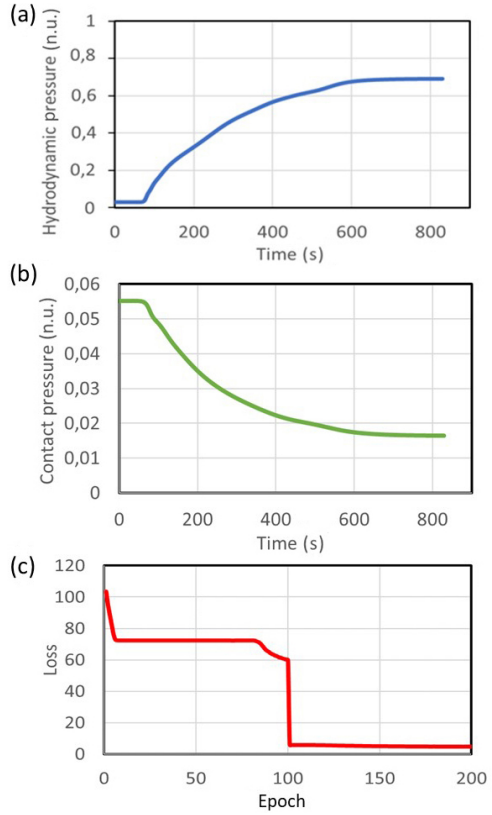

Fig. 5 Results of ANN prediction of evolution of pressure during the friction process. (a) Prediction of hydrodynamic pressure p_h; (b) prediction of contact pressure p_s; (c) loss function calculated during epoch loop.

friction process. As the contact pressure non-linear decreases, the hydrodynamic pressure increases in similar pattern. It should be noted that the non-linearity was not provided by any of the equations used for error estimation. The non-linear behaviour with time was found from the input experimental data. This feature was successfully "extracted" during the optimization process and "transfered" to the predictions by the ANN pressure evolution.

The presented ANN structure and data-driven optimization method is not limited to evaluate the the non-linear relationship between input time series t and the output wear rate $\dot{w}(t)$ or pressure $p(t)$ under a specific test condition. The effects of test conditions on the ANN structure can also be taken into account. There are two ways to incorparate test conditions. One is to use an additional set of coallocation points, let it be an additional vector of the state denoted as f, as a secondary axis of the input data. In this way, ANN will generate a map according variables (t, f). Hovewer, this way requires to provide the information that defines how the experimental data depend on the friction/wear state f. The second way is to add an additional MLP corresponding to the wear/pressure state to be evaluated $\hat{\varphi} \mapsto \mathcal{N}_{\varphi}(t, \boldsymbol{W}, \boldsymbol{b})$ and add the new term to the loss function denoting the constitutive law (can also be purely empirical) for the wear/pressure state to be investigated. Such extensions are left for investigations and verifications in the future.

5 Conclusions

In this study, we have examined an ANN consisting of several parallel MLPs, with data-driven optimization procedure, to estimate the contact and hydrodynamic pressure in mixed lubrication regime of friction. The equations for ANN prediction are based on simple physical relationships that allow the unknown solution (dependence) of the function to be approximated by the two or more MLPs. One of the MLPs acts as a prior on the unknown relationship between experimental and predicted data, the other works as an approximation to the spatiotemporal dependence.

The major achievement of such an ANN structure is the ability to feed the experimental data directly into the modified loss function allowing the prediction of the output data with reference to the input data. The time series with constant increment was used as input data for a first neural layer of the MLP, and this time series data was used as vector of collocation points for the pressure output data (the last neural layer in the MLP), which allows the pressure to be reconstructed as a function of time. We pointed out that the underlying reason for this behavior is the particular architecture of the network, where the input variables are only the spatial or temporal dimensions, allowing the network output data to adapt to the required variability needed for gradient-based optimization, to best predict the set of output data.

This type of ANN with data-driven optimizer allows the prediction of "hidden" tribological laws or dependencies that are not obvious or cannot be measured directly regardless to the test scheme selected. We find that the optimizer performs much better at accessing the relationship between experimental

data and the set of equations where the relationship exists explicitly for functions, and provides excellent opportunities to study tribological properties using artificial neural network, deep learning, and machine learning techniques.

Acknowledgements

This work was funded by the National Natural Science Foundation of China (NSFC) with Grant No. 51635009.

Declaration of competing interest

The authors have no competing interests to declare that are relevant to the content of this article. The author Yu TIAN is the Editorial Board Member of this journal. The author Yonggang MENG is the Associate Editor of this journal.

References

[1] Kelleher J D, Mac Namee B, and D'Arcy A. *Fundamentals of Machine Learning for Predictive Data Analytics*. The MIT Press, 2015.

[2] Marian M, Tremmel S. Current trends and applications of machine learning in tribology—A review. *Lubricants* **9**(9): 86 (2021)

[3] Rosenkranz A, Marian M, Profito F J, Aragon N, Shah R. The use of artificial intelligence in tribology—A perspective. *Lubricants* **9**(1): 2 (2020)

[4] Singh J, Azamfar M, Li F, Lee J. A systematic review of machine learning algorithms for prognostics and health management of rolling element bearings: Fundamentals, concepts and applications. *Meas Sci Technol* **32**(1): 012001 (2020)

[5] Hamadache M, Jung J H, Park J, Youn B D. A comprehensive review of artificial intelligence-based approaches for rolling element bearing PHM: Shallow and deep learning. *JMST Adv* **1**(1–2): 125–151 (2019)

[6] Argatov I. Artificial neural networks (ANNs) as a novel modeling technique in tribology. *Front Mech Eng* **5**: 30 (2019)

[7] Zhang Z N, Yin N, Chen S, Liu C L. Tribo-informatics: Concept, architecture, and case study. *Friction* **9**(3): 642–655 (2021)

[8] Zhang Y Z, Kovalev A, Hayashi N, Nishiura K, Meng Y G. Numerical prediction of surface wear and roughness parameters during running-in for line contacts under mixed lubrication. *J Tribol* **140**(6): 061501 (2018)

[9] Maier M, Pusterhofer M, Grün F. Wear simulation in lubricated contacts considering wear-dependent surface topography changes. *Mater Today Proc* **93**: 563–570 (2023)

[10] Sander D E, Allmaier H, Priebsch H H, Witt M, Skiadas A. Simulation of journal bearing friction in severe mixed lubrication—Validation and effect of surface smoothing due to running-in. *Tribol Int* **96**: 173–183 (2016)

[11] Patir N, Cheng M S. Application of average flow model to lubrication between rough sliding surfaces. *J Lubr Technol* **101**(2): 220–229 (1979)

[12] Meng Y G, Xu J, Jin Z M, Prakash B, Hu Y Z. A review of recent advances in tribology. *Friction* **8**(2): 221–300 (2020)

[13] Meng Y G, Xu J, Ma L R, Jin Z M, Prakash B, Ma T B, Wang W Z. A review of advances in tribology in 2020–2021. *Friction* **10**(10): 1443–1595 (2022)

[14] Habchi W. *Finite Element Modelling of Elastohydrodynamic Lubrication Problems*. Wiley, 2018.

[15] Ruggiero A, Sicilia A. Implementation of a finite element deformation model within an elasto-hydrodynamic lubrication numerical solver for a ball in socket tribopair. *Front Mech Eng* **8**: 909156 (2022)

[16] Liu W K, Hu Y K. Finite element hydrodynamic friction model for metal forming. *Numerical Meth Engineering* **37**(23): 4015–4037 (1994)

[17] Lubrecht A A, Venner C H, Colin F. Film thickness calculation in elasto-hydrodynamic lubricated line and elliptical contacts: The Dowson, Higginson, Hamrock contribution. *Proc Inst Mech Eng Part J J Eng Tribol* **223**(3): 511–515 (2009)

[18] Evans C R, Johnson K L. The rheological properties of elastohydrodynamic lubricants. *Proc Inst Mech Eng Part C J Mech Eng Sci* **200**(5): 303–312 (1986)

[19] Onions R A, Archard J F. The contact of surfaces having a random structure. *J Phys D*: *Appl Phys* **6**(3): 289–304 (1973)

[20] Greenwood J A, Williamson J B P. Contact of nominally flat surfaces. *Proceedings of the Royal Society of London. Series A, Mathematical and Physical Sciences* **295**(1442): 300–319 (1966)

[21] Çetinel H, Öztürk H, Çelik E, Karlık B. Artificial neural network-based prediction technique for wear loss quantities in Mo coatings. *Wear* **261**(10): 1064–1068 (2006)

[22] Kumar S, Priyadarshan, Ghosh S K. Statistical and artificial neural network technique for prediction of performance in $AlSi_{10}Mg$-MWCNT based composite materials. *Mater Chem Phys* **273**: 125136 (2021)

[23] Becker A, Fals H D C, Roca A S, Siqueira I B A F, Caliari F R, da Cruz J R, Vaz R F, de Sousa M J, Pukasiewicz A G M. Artificial neural networks applied to the analysis of performance and wear resistance of binary coatings $Cr_3C_2$37WC18M and WC20$Cr_3C_2$7Ni. *Wear* **477**: 203797 (2021)

[24] Argatov I I, Chai Y S. Artificial neural network modeling of sliding wear. *Proc Inst Mech Eng Part J J Eng Tribol* **235**(4): 748–757 (2021)

[25] Altay O, Gurgenc T, Ulas M, Özel C. Prediction of wear loss quantities of ferro-alloy coating using different machine learning algorithms. *Friction* **8**(1): 107–114 (2020)

[26] Ulas M, Altay O, Gurgenc T, Özel C. A new approach for prediction of the wear loss of PTA surface coatings using artificial neural network and basic, kernel-based, and weighted extreme learning machine. *Friction* **8**(6): 1102–1116 (2020)

[27] Sardar S, Dey S, Das D. Modelling of tribological responses of composites using integrated ANN-GA technique. *J Compos Mater* **55**(7): 873–896 (2021)

[28] Jesuthanam C P, Kumanan S, Asokan P. Surface roughness prediction using hybrid neural networks. *Mach Sci Technol* **11**(2): 271–286 (2007)

[29] Iriaye E F, Ighravwe D E, Alade A O, Afolalu S A, Adelakun O J. Development of artificial neural network for surface roughness and machine prediction. *J Phys*: *Conf Ser* **1378**: 042034 (2019)

[30] Jones S P, Jansen R, Fusaro R L. Preliminary investigation of neural network techniques to predict tribological properties. *Tribol Trans* **40**(2): 312–320 (1997)

[31] Baydoun S, Fartas M, Fouvry S. Comparison between physical and machine learning modeling to predict fretting wear volume. *Tribol Int* **177**: 107936 (2023)

[32] Raissi M, Perdikaris P, Karniadakis G E. Physics-informed neural networks: A deep learning framework for solving forward and inverse problems involving nonlinear partial differential equations. *J Comput Phys* **378**: 686–707 (2019)

[33] Raissi M, Yazdani A, Karniadakis G E. Hidden fluid mechanics: Learning velocity and pressure fields from flow visualizations. *Science* **367**(6481): 1026–1030 (2020)

[34] Haghighat E, Raissi M, Moure A, Gomez H, Juanes R. A deep learning framework for solution and discovery in solid mechanics. *arXiv*: 2003.02751 (2020)

[35] Rudy S, Alla A, Brunton S L, Kutz J N. Data-driven identification of parametric partial differential equations. *SIAM J Appl Dyn Syst* **18**(2): 643–660 (2019)

[36] Weeks B L, Ruddle C M, Zaug J M, Cook D J. Monitoring high-temperature solid–solid phase transitions of HMX with atomic force microscopy. *Ultramicroscopy* 93(1): 19–23 (2002)

[37] Haghighat E, Juanes R. SciANN: A Keras/TensorFlow wrapper for scientific computations and physics-informed deep learning using artificial neural networks. *Comput Meth Appl Mech Eng* **373**: 113552 (2021)

[38] Zubov K, McCarthy Z, Ma Y B, Calisto F, Pagliarino V, Azeglio S, Bottero L, Luján E, Sulzer V, Bharambe A, *et al*. NeuralPDE: Automating physics-informed neural networks (PINNs) with error approximations. *arXiv*: 2107.09443 (2021)

[39] Almqvist A. Fundamentals of physics-informed neural networks applied to solve the Reynolds boundary value problem. *Lubricants* **9**(8): 82 (2021)

[40] Wang N Z, Tsai C M. Assessment of artificial neural network for thermohydrodynamic lubrication analysis. *Ind Lubr Tribol* **72**(10): 1233–1238 (2020)

[41] Marian M, Mursak J, Bartz M, Profito F J, Rosenkranz A, Wartzack S. Predicting EHL film thickness parameters by machine learning approaches. *Friction* **11**(6): 992–1013 (2023)

[42] Nascimento R G, Viana F A C. Fleet prognosis with physics-informed recurrent neural networks. In *Structural Health Monitoring 2019: Enabling Intelligent Life-Cycle Health Management for Industry Internet of Things (IIOT)*. Chang F K, Kopsaftopoulos F, Eds., 2019: doi: 10.12783/shm2019/32301.

[43] Nascimento R G, Viana F A C. Cumulative damage modeling with recurrent neural networks. *AIAA J* **58**(12): 5459–5471 (2020)

[44] Dourado A, Viana F A C. Physics-informed neural networks for missing physics estimation in cumulative damage models: A case study in corrosion fatigue. *J Comput Inf Sci Eng* **20**(6): 061007 (2020)

[45] Magoulas G D, Vrahatis M N. Adaptive algorithms for neural network supervised learning: A deterministic optimization approach. *Int J Bifurcation Chaos* **16**(7): 1929–1950 (2006)

[46] Oussar Y, Dreyfus G. How to be a gray box: Dynamic semi-physical modeling. *Neural Netw* **14**(9): 1161–1172 (2001)

[47] Forssell U, Lindskog P. Combining semi-physical and neural network modeling: An example ofIts usefulness. *IFAC Proc Vol* **30**(11): 767–770 (1997)

[48] Haviez L, Toscano R, El Youssef M, Fouvry S, Yantio G, Moreau G. Semi-physical neural network model for fretting wear estimation. *J Intell Fuzzy Syst Appl Eng Technol* **28**(4): 1745–1753 (2015)

[49] Haykin S. *Neural Networks: A Comprehensive Foundation*. Prentice Hall PTR, 1998.

[50] Bergstra J, Bardenet R, Bengio Y, Kégl B. Algorithms for hyper-parameter optimization. In Proceedings of the 24th International Conference on Neural Information Processing Systems, 2011: 2546–2554.

[51] Kingma D P, Ba J L. Adam: A method for stochastic optimization. *ArXiv*: https://arxiv.org/abs/1412.6980v9 (2023)

[52] Bowden F P, Tabor D. 1964 *The Friction and Lubrication of Solids*. Oxford: Clarendon Press.

[53] Bair S, Winer W O. A rheological model for elastohydrodynamic contacts based on primary laboratory data. *J Lubr Technol* 101(3): 258–264.

[54] Hsu S M, Munro R G, Shen M C, Gates R S. Boundary Lubricated Wear. In: *Wear—Materials, Mechanisms and Practice*. Stachowiak G, Ed. Chichester (UK), John Wiley & Sons Ltd., 2014: 37–70.

[55] Walker J, Questa H, Raman A, Ahmed M, Mohammadpour M, Bewsher S R, Offner G. Application of tribological artificial neural networks in machine elements. *Tribol Lett* **71**(1): 1–16 (2022)

[56] Archard J F. Contact and rubbing of flat surfaces. *J Appl Phys* **24**(8): 981–988 (1953)

[57] Hsu S M. Boundary lubrication of materials. *MRS Bull* **16**(10): 54–58 (1991)

[58] Hsu S M, Shen M C, Ruff A W. Wear prediction for metals. *Tribol Int* **30**(5): 377–383 (1997)

[59] Friedrich K, Reinicke R, Zhang Z. Wear of polymer composites. *Proc Inst Mech Eng Part J J Eng Tribol* **216**(6): 415–426 (2002)

[60] Rice J R, Ruina A L. Stability of steady frictional slipping. *J Appl Mech* **50**(2): 343–349 (1983)

[61] Bowden F P, Leben L. Nature of sliding and the analysis of friction. *Nature* **141**: 691–692 (1938)

[62] Velten K, Reinicke R, Friedrich K. Wear volume prediction with artificial neural networks. *Tribol Int* **33**(10): 731–736 (2000)

[63] Argatov I I, Chai Y S. An artificial neural network supported regression model for wear rate. *Tribol Int* **138**: 211–214 (2019)

[64] Zhang Y Z, Kovalev A, Meng Y G. Combined effect of boundary layer formation and surface smoothing on friction and wear rate of lubricated point contacts during normal running-in processes. *Friction* **6**(3): 274–288 (2018)

[65] Yao H H, Zhou Z, Wang L, Tan Z, He D Y, Zhao L D. Thermal conductivity and wear behavior of HVOF-sprayed Fe-based amorphous coatings. *Coatings* **7**(10): 173 (2017)

[66] Ruina A. Slip instability and state variable friction laws. *J Geophys Res* **88**(B12): 10359–10370 (1983)

Alexander KOVALEV. He received his M.S. degree in physics from the Gomel State University, Belarus, in 1997. He has earned Ph.D. degree in tribology and physics of solids in 2007 from Metal-Polymer Research Institute, Gomel, Belarus. He had a position as a research fellow in 2016–2018 and 2021–2022 at State Key Laboratory of Tribology in Advanced Equipment at Tsinghua University, China. His field of research concentrates on micro/nano-tribology, contact mechanics, and interfacial phenomena. He employs the modern research methods, such as machine and deep learning, to analyze tribological characteristics.

Yu TIAN. He gained his B.S. and Ph.D. degrees in mechanical engineering at Tsinghua University, China, in 1998 and 2002, respectively. His current position is a professor and deputy director of the State Key Laboratory of Tribology in Advanced Equipment (SKLT) at Tsinghua University. His research interest is the science and technology at the interface of physics, materials, engineering, and biology, the mechanism of adhesion, friction, and lubrication and their active control.

Yonggang MENG. He received his M.S. and Ph.D. degrees in mechanical engineering from Kumamoto University, Japan, in 1986 and 1989 respectively. He joined the State Key Laboratory of Tribology (renamed as State Key Laboratory of Tribology of Advanced Equipment since 2022) at Tsinghua University, China, from 1990. His research areas cover the tribological design of machine components, MEMS devices and Hard Disk Drives as well as active control of friction and interfacial phenomena.